

# Double-Peaked Electrostatic Ion Cyclotron Harmonic Waves

S. A. BOARDSEN<sup>1</sup> AND D. A. GURNETT

*Department of Physics and Astronomy, University of Iowa, Iowa City*

W. K. PETERSON

*Research and Development, Lockheed, Palo Alto, California*

Electrostatic  $H^+$  cyclotron harmonic waves are often observed along the auroral field lines at altitudes of 1–3.5  $R_E$  by the Dynamics Explorer 1 satellite. A small fraction of these waves are found to have two peaks associated with each harmonic instead of one peak. The waves occur below the lower hybrid frequency and are usually relatively weak, about a factor of 4 smaller than typical electric field amplitudes of other  $H^+$  cyclotron harmonic wave events. For two events the separation between the spectral peaks is found to be proportional to the harmonic number. The double-peaked spectral signature is believed to be produced by Doppler shifts arising from the satellite velocity relative to the plasma rest frame. The wavelength and phase velocity of the harmonics can be determined by measuring the separation between the peaks. The waves were found to have wavelengths of the order of 300 m and phase velocities of the order of 150 km/s. The proportionality between the peak separation and the harmonic number indicates that the phase velocity is approximately constant, independent of harmonic number. Assuming that the phase velocity is constant, it is shown that as  $\Delta k/k$  increases, the double peaks merge to form a single spectral peak. For the wave events presented in this paper,  $\Delta k/k$  is estimated to be less than 0.1.

## 1. INTRODUCTION

Electrostatic  $H^+$  cyclotron harmonic waves are frequently observed by the Dynamics Explorer 1 (DE 1) spacecraft. These waves typically occur near the higher harmonics (typically  $n > 5$ ) of the  $H^+$  cyclotron frequency  $f_{H^+} = (\frac{1}{2}\pi) (eB/mc)$  [Kintner, 1980]. In about one out of 10  $H^+$  cyclotron harmonic wave observations made by DE 1 the  $H^+$  cyclotron emissions take on a double-peaked characteristic. The purpose of this paper is to describe the double-peak structure of the  $H^+$  cyclotron harmonic emissions and discuss their interpretation. The double-peak structure is interpreted in terms of the Doppler shift arising from the satellite's velocity relative to the plasma's rest frame. Kintner *et al.* [1978] discussed the broadening of electrostatic  $H^+$  cyclotron waves in terms of Doppler shifts and used the broadening to estimate a lower limit for the phase velocity of the waves. As we will show, harmonics with a double-peaked structure can be used to obtain more precise estimates of the phase velocity.

DE 1 is in an ideal orbit for studying ion cyclotron harmonic waves along the auroral field lines. This spacecraft is in a polar orbit about the Earth with apogee and perigee geocentric radial distances of 4.67  $R_E$  and 1.106  $R_E$ . The orbital period is roughly 7 hours. The spacecraft spin axis is perpendicular to the orbital plane, and the spacecraft rotates with a period of roughly 6 s. A 215-m electric antenna ( $E_x$ ), oriented perpendicular to the spin axis, is used to detect the electric field of the ion cyclotron harmonic waves. A wide-band receiver is used to provide high-resolution spectrograms of ion cyclotron harmonic waves. For a description of

the plasma wave instrument on DE 1, see *Shawhan et al.* [1981]. The rest of this paper is divided into three sections. Section 2 presents observations of double-peaked  $H^+$  cyclotron harmonic waves. Section 3 presents our interpretation of the cause of the double-peaked harmonics, and section 4 summarizes the conclusion of the study.

## 2. OBSERVATIONS OF DOUBLE-PEAKED HARMONICS

Two double-peaked  $H^+$  cyclotron harmonic wave events will be discussed. The first event is the more typical of the double-peaked  $H^+$  cyclotron harmonic wave events found. In these events two to three harmonics are excited at high harmonic numbers ( $n \approx 10$ ). The second event is less typical and shows an event in which the double-peaked harmonics occur at lower harmonic numbers ( $n \sim 3-7$ ). Two events have been found in which the separation between the peaks is clearly observed to be proportional to the harmonic number. The proportional relationship has only been observed in events that occur at low harmonic numbers.

The first double-peaked  $H^+$  cyclotron harmonic wave event that will be discussed covers a series of  $H^+$  cyclotron harmonic emissions that started at approximately 0353 UT and ended at 0358 UT on June 1, 1984. During this event the radial distance varied from 2.67  $R_E$  to 2.84  $R_E$  and the invariant latitude varied from 73.2° to 75.9°. The magnetic local time was about 16 hours. A spectrogram of the  $H^+$  cyclotron harmonic event is shown in Figure 1. The  $H^+$  cyclotron harmonics are first clearly observed at 0353:06 UT at around 600 Hz. The  $H^+$  cyclotron harmonics during this time interval show no double peaks. The twelfth through sixteenth harmonics are excited. The intensities peak at frequencies slightly below  $n f_{H^+}$ .

The  $H^+$  harmonics first become double-peaked at about 0354 UT. Instead of each harmonic occurring at one frequency (represented by a single line in the spectrogram), each harmonic occurs at two frequencies (represented by

<sup>1</sup>Now at NASA Marshall Space Flight Center, Huntsville, Alabama.

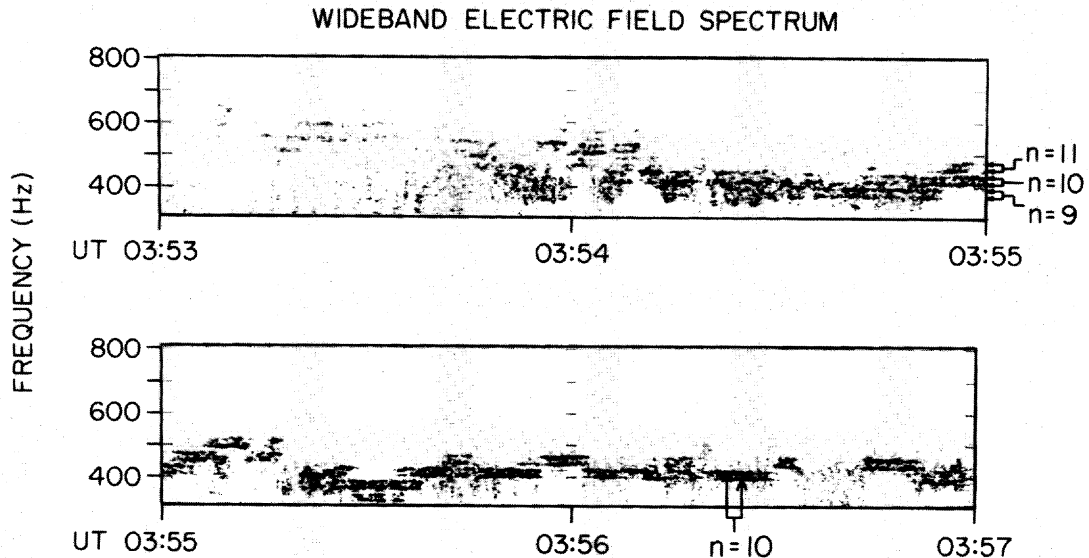


Fig. 1. A spectrogram of the analog wideband electric field signal detected by the  $E_x$  antenna on DE 1 in the 0–1 kHz mode. Double-peaked  $H^+$  harmonics are present between 300 and 600 Hz. The ninth, tenth, and eleventh harmonics are indicated by arrows.

two closely spaced lines in the spectrogram as indicated in Figure 1). Figure 2a shows a spectrum covering the time interval 0354:50–0355:00.3 UT. The vertical lines are spaced at integer multiples of the  $H^+$  cyclotron frequency as determined by the DE 1 magnetometer. Note that the ninth through eleventh harmonics are excited and that each harmonic shows a distinct double peak. In Figure 2b only the tenth harmonic is excited. The average frequency of each harmonic occurs at a frequency slightly above  $n f_{H^+}$ . In a theoretical study by Andre [1986] the  $H^+$  cyclotron harmonics also occur close to  $n f_{H^+}$ . Positive perpendicular slopes of a  $H^+$  loss cone distribution drove the instability in his study.

The particle data from the energetic ion composition spectrometer (EICS) indicates that a loss cone feature (Figure 3a) is observed in the  $H^+$  ions during this event; the location of the atmospheric loss cone is indicated by dashed lines. The loss cone appears 16 min before the event begins and ends 3 min after the event ends. A similar observation was made by Koskinen *et al.* [1987]. A plot (Figure 3b) of the log of the phase space density versus energy for  $H^+$  indicates that a  $\sim 90$  eV component and a very hot energetic component (which makes up less than 1% of the  $H^+$ ) is present in the  $H^+$  ion distribution. We find that above the 10 eV EICS threshold the plasma is dominated by  $H^+$ .  $O^+$  accounts for less than 10% of the ion plasma. From EICS data alone we estimate that the total density from ions with energies 10 eV above the spacecraft potential is  $\sim 1 \text{ cm}^{-3}$ .

For theoretical modeling it is important to estimate the location of the lower hybrid frequency. Unfortunately, we could not use the method of Persoon *et al.* [1988] to make an accurate determination of the total plasma density because of the lack of a sharp upper frequency cutoff of the auroral hiss. Also, the wave event lies equatorward of the source region of the hiss and therefore in the region where the whistler mode does not reach resonance [Persoon *et al.*, 1988]. This means that an observed cutoff in the hiss would underestimate the plasma density. The highest frequency at

which auroral hiss is observed during this event is 20 kHz, and therefore a lower limit can be placed on the plasma density of  $5 \text{ cm}^{-3}$ . The lower limit on the lower hybrid frequency is estimated to be 455 Hz for a plasma consisting of only  $H^+$  and 435 Hz if 10% of the plasma is composed of  $O^+$ . Therefore the  $H^+$  cyclotron harmonic waves are located below the lower hybrid frequency. In the theoretical study by Andre [1986] it is shown that a broadband emission can occur below but close to the lower hybrid frequency. A broadband emission is also observed in the wave data (not shown). At the start of the event a broadband emission is centered around 300 Hz and gradually increases to 400 Hz when the double-peaked harmonics occur. The band persists until the loss cone disappears at 0401 UT (not shown). This broadbanded feature could indicate that the actual lower hybrid frequency is close to the lower limit that we have placed on it.

The  $H^+$  cyclotron harmonics are strongly spin modulated. This modulation is not easily detected in the spectrogram due to the logarithmic compression of the data by the wideband receiver. However, it is clearly evident in plots of the rms electric field strength in the 10-Hz to 1-kHz band. Figure 4 shows a plot of the rms electric field strength versus time over the interval 0355 UT to 0356 UT. The dashed vertical lines in the plot indicate when the  $E_x$  antenna is parallel to the magnetic field. This plot can be used to estimate  $k_{\parallel}/k_{\perp}$  since the  $H^+$  cyclotron harmonics make the dominant contribution to the rms electric field strength (see Figures 2a and 2b). The ratio  $k_{\parallel}/k_{\perp}$  is estimated to be less than 0.2. The rms electric field amplitude associated with the single-peaked  $H^+$  cyclotron harmonics that occur between 035306 UT and 035350 UT (Figure 1) is approximately 0.15 mV/m, while the rms electric field amplitude associated with the double-peaked harmonics that occur after 0354 UT is 0.26 mV/m.

The second double-peaked  $H^+$  cyclotron harmonic wave event that we will discuss occurred on January 15, 1984,

from 104510 UT to 104550 UT. During this event the radial distance was about  $2.6 R_E$ , and the invariant latitude was about  $75.8^\circ$ . The magnetic local time was about 16.5 hours. A frequency spectrum taken from this event is shown in Figure 5a. The third to the seventh harmonics (indicated by arrows) are double-peaked. Notice that the separation between the double peaks increases with harmonic number. This separation is roughly proportional to harmonic number. This relationship is illustrated in Figure 5b. The ordinate (in units of inverse kilometer) is proportional to frequency separation between the double peaks (this proportionality will be derived in section 3), and the abscissa is the measured average frequency of the double-peaked harmonics (which is proportional to harmonic number). The measured values for each harmonic are plotted (triangles), indicating an approximately linear relationship between the frequency separation and the harmonic number.

The EICS instrument indicates that a loss cone feature (not shown) is also observed in the  $H^+$  ions for this event. There is a net flux of  $H^+$  ions ( $>10$  eV above spacecraft potential) flowing down the field lines. The  $H^+$  thermal energy for this event is  $\sim 90$  eV as determined by EICS. The

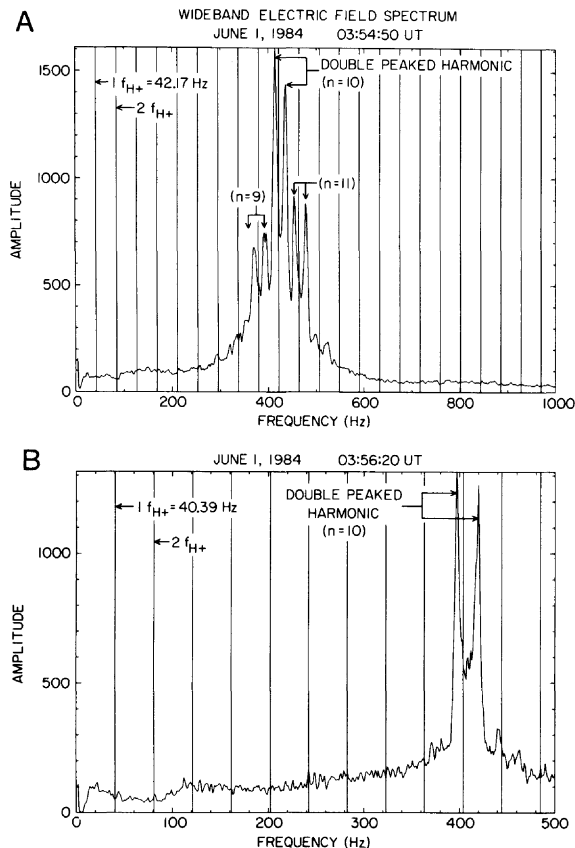


Fig. 2. (a) A spectrum of the analog wideband electric field signal taken on June 1, 1984, at 035450 UT consisting of 250 spectrums averaged over 12.5 s. The ninth through eleventh harmonics are excited, and each one is double-peaked. The evenly spaced lines are located at integer multiples of the  $H^+$  cyclotron frequency. (b) A spectrum consisting of 250 spectrums averaged over 12.5 s taken on June 1, 1984, at 035620 UT.

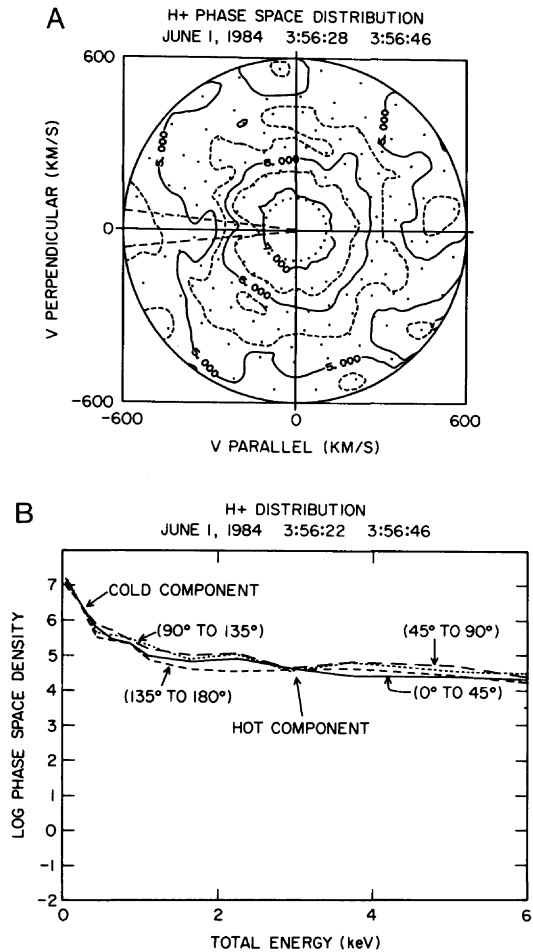


Fig. 3. (a) A plot of  $H^+$  distribution function measured by EICS on June 1, 1984, at 35628–46 UT. The solid contours are spaced at the decade intervals of the phase space density measured in units of  $s^3 km^{-6}$ . The dashed curves are at half-decade intervals. Particles with a positive parallel velocity are flowing toward the ionosphere. The dashed lines indicate the location of atmospheric loss cone. (b) A plot of the log of the phase space density versus energy for  $H^+$  during the wave event. Each curve refers to a different range of pitch angles that the detector was sampling.

estimated  $H^+$  density ( $>10$  eV above the spacecraft's potential) is  $\sim 2 cm^{-3}$ . A significant cold ion background population is also present for this event. The upper frequency limit of the auroral hiss is hard to identify for this case, but hiss appears to be present at 20 kHz. The event also occurs on field lines equatorward of the source of the hiss emissions. Therefore we place a lower limit on the density of  $5 cm^{-3}$ .

These waves are also strongly spin modulated with the peak electric field amplitudes occurring when the  $E_x$  antenna is perpendicular to the magnetic field. The rms electric field amplitude associated with these waves is 0.4 mV/M.

We believe that the double-peaked harmonics are due to the Doppler shift arising from the relative velocity between the satellite and the plasma. In section 3 we will show how the Doppler shift can cause double-peaked harmonics. A simple relationship will be derived relating the frequency

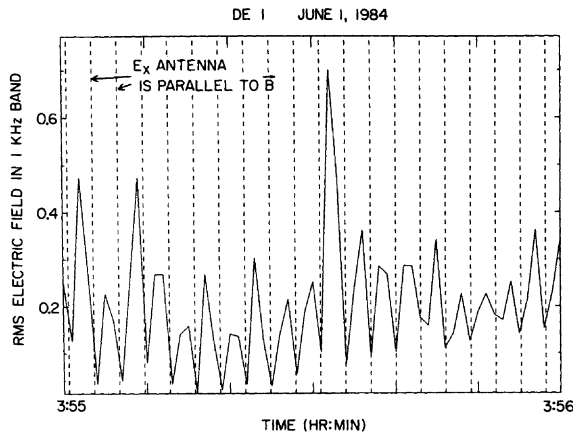


Fig. 4. The rms electric field in the 10-Hz to 1-kHz band measured by the  $E_x$  antenna versus time. The dashed vertical lines indicate when the  $E_x$  antenna is parallel to the magnetic field.

separation of the double peaks to the wavelength of the harmonics. This relationship when applied to the observed frequency spectrums is used to show that the phase velocity is roughly independent of harmonic number. Assuming that the phase velocity is constant, it will then be shown that as the spread in unstable wave numbers ( $\Delta k_{\perp}$ ) increases, for a given harmonic the double peaks merge into a signal spectral peak. In most cases, double-peaked structures are not detected in electrostatic  $H^+$  cyclotron wave events (i.e., events with wave power peaking in the first harmonic). A brief discussion of the lack of double-peaked harmonic observations for electrostatic  $H^+$  cyclotron waves will be given at the end of section 3.

### 3. INTERPRETATION OF DOUBLE-PEAKED HARMONICS

To introduce the basic idea, a simple heuristic discussion will first be used to show how Doppler shifts can cause double-peaked harmonics. The basic geometry involved is shown in Figure 6. By design the  $E_x$  antenna was chosen to rotate in the plane defined by magnetic field direction and the satellite velocity direction. The electric fields and wave vectors of the electrostatic  $H^+$  cyclotron harmonic waves are assumed to be oriented almost perpendicular to the magnetic field, and distributed gyrotropically around the magnetic field lines. A gyrotropic distribution is expected because the wavelength of the waves is much smaller than the spatial structure of the region in which the waves occur. As discussed earlier, the waves are observed to occur almost continuously for about a 1-min interval which corresponds to a distance of 240 km transverse to the magnetic field, and the wavelengths of the waves (as will be determined later in this section) are only about 300 m.

The projection of an electric field  $E_{\perp}$ , making at an angle of  $\phi$  with respect to the component of the satellite velocity perpendicular to the magnetic field  $V_{\perp}$ , onto the  $E_x$  antenna is  $E_{\perp} \sin(\alpha t) \cos(\phi)$ , where  $\alpha$  is the angular spin rate of the satellite. The contribution made by electrostatic waves traveling in a direction  $\phi$  (see Figure 6) to the net signal is seen to be weighted by a  $\cos(\phi)$  factor (since for electrostatic waves  $E \parallel k$ ). Therefore the waves traveling in directions

almost perpendicular to  $V_{\perp}$  make almost no contribution to the signal. On the other hand, waves traveling almost parallel or antiparallel to  $V_{\perp}$  make a large contribution to the signal. If  $\Delta k/k$  is small, the waves traveling in the direction of  $V_{\perp}$  will contribute a spectral peak that is downshifted in frequency by  $V_{\perp}/\lambda$ , and the waves traveling in the opposite direction of  $V_{\perp}$  will contribute a spectral peak that is upshifted in frequency by  $V_{\perp}/\lambda$ . If other factors contributing to spectral peak broadening are sufficiently small, a double-peaked spectrum will be observed with a frequency separation given approximately by

$$\Delta f = 2V \sin \theta / \lambda \quad (1)$$

where  $V$  is the magnitude of the satellite velocity and  $\theta$  is the angle between the satellite velocity and the magnetic field direction.

Table 1 lists the inferred wavelengths and perpendicular phase velocities determined by measuring the separation of the double peaks for the spectra in Figures 2a and 2b. The ninth and tenth harmonics have the same phase velocity, while the eleventh harmonic has a slightly higher phase velocity. For the January 15 event the inferred inverse wavelengths and average frequencies of the third to the seventh harmonics are plotted (Figure 5b). The plotted

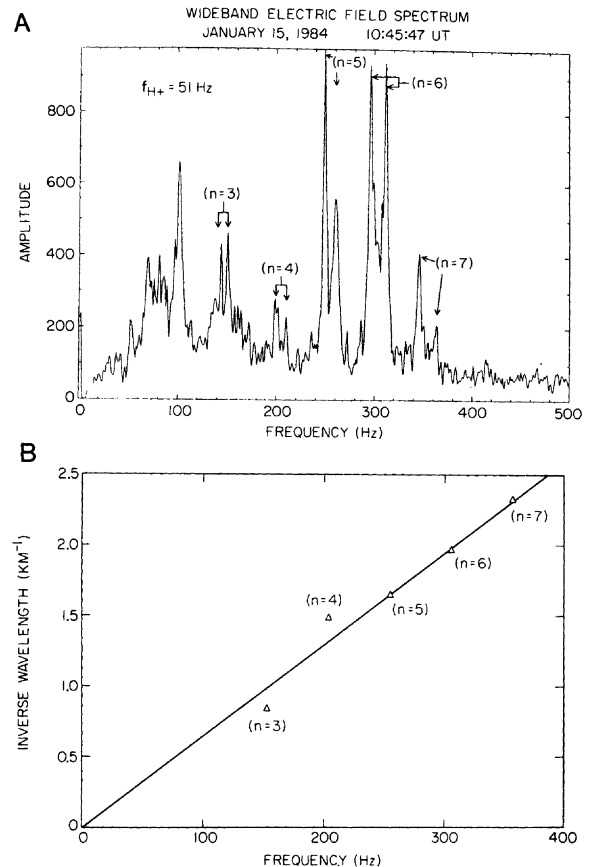


Fig. 5. (a) A spectrum taken on January 15, 1984, where the third to the seventh harmonics are excited. (b) A plot of the inferred inverse wavelengths versus the center frequencies for the excited harmonics shown in Figure 8a.

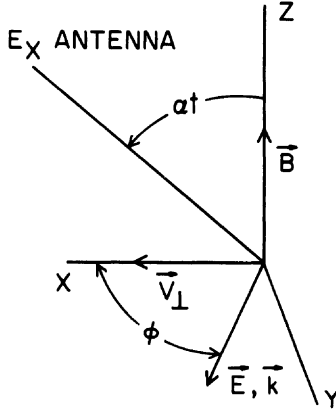


Fig. 6. The orientation of the  $E_x$  antenna with respect to the electric field of the waves is shown. The  $E_x$  antenna rotates in the plane defined by  $\mathbf{B}$  and the perpendicular component of the satellite velocity  $\mathbf{V}_\perp$ , while the electric fields lie mainly in the plane perpendicular to  $\mathbf{B}$ .

points suggest that a linear relationship exists between inverse wavelength and frequency. This relationship indicates that the phase velocity is approximately constant  $\sim 153$  km/s, independent of harmonic number.

The inferred phase velocities for the two events presented are in good agreement with the thermal velocity of the simultaneously measured  $\text{H}^+$  component by EICS. The EICS instrument measures only ions with energies  $>10$  eV above the spacecraft potential. For a plasma density of  $5 \text{ cm}^{-3}$ , the spacecraft potential is typically between 4 and 8 eV [Chappell, 1988]. For the June 1 case the upper cutoff of the auroral hiss indicates that a substantially lower energy component is present that makes up at least 80% of the plasma. If this component has a temperature of 1 eV, its thermal velocity is 10 times smaller than the inferred phase velocities of the ion cyclotron harmonic waves. If the phase velocity is much larger than the  $\text{H}^+$  thermal velocity, the real part of the dispersion relationship can probably be approximated by the fluid limit. Therefore for the higher harmonics the phase velocities of the harmonics should be approximately constant and close to the ion acoustic velocity. Unfortunately, the high-altitude plasma instrument (HAPI), which measures electrons, failed before low-frequency (0–1 kHz) wideband wave data became available. Consequently, no experimental determination of the electron temperature can be made, and hence the ion acoustic velocity cannot be determined.

TABLE 1. Measured Perpendicular Phase Velocities of Harmonics

Harmonic	$\Delta f$ , Hz	$f_0$ , Hz	$\lambda$ , m	$V\phi$ , km/s
<i>0354:50–0355:02.5 UT</i>				
Ninth	20.7	382.15	362	138
Tenth	23.0	424.7	326	138
Eleventh	23.0	466.1	326	152
<i>0356:20–0356:32.5 UT</i>				
Tenth	23.0	407.8	326	134

The parameters are  $\theta = 51.115^\circ$ ;  $V_{\text{sat}} = 4.82$  km/s;  $\lambda = 2V_{\text{sat}} \sin \theta / \Delta f$ ; and  $\Delta f$  is the separation between the split harmonic peaks.

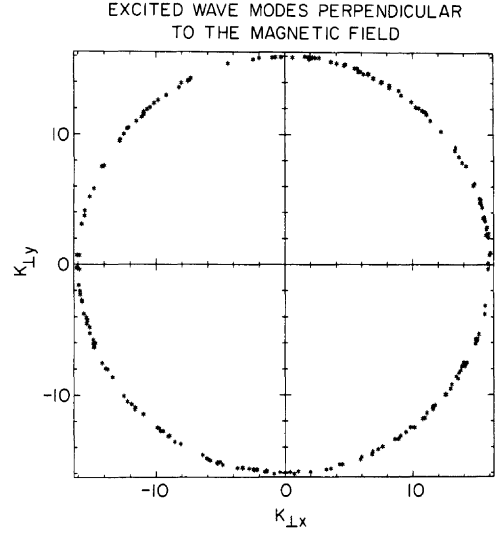


Fig. 7. A plot of randomly selected perpendicular wave numbers lying in an annular ring of width  $2\Delta k_{\perp 0}$ , centered at  $k_{\perp 0}$ .

One of the criteria that must be satisfied in order to observe double-peaked harmonics is that  $\Delta k/k$  must be sufficiently small. To first order,  $\omega(\mathbf{k})$  can be approximated by  $\omega(\mathbf{k}) = \omega(\mathbf{k}_0) + \mathbf{V}_g \cdot (\mathbf{k} - \mathbf{k}_0)$ , where  $\mathbf{V}_g = \partial\omega/\partial\mathbf{k}|_{\mathbf{k}_0}$  is the group velocity. Therefore the spectral broadening due to the frequency dispersion relation is  $\mathbf{V}_g \cdot \Delta\mathbf{k}$ . The double peaks will become obscured when  $\mathbf{V}_g \cdot \Delta\mathbf{k}$  becomes as large in magnitude as the separation in frequency of the double peaks predicted by (1). Therefore the following condition must be satisfied in order to observe double-peaked harmonics:

$$\Delta k/k < 2V \sin \theta / V_g \quad (2)$$

Assuming that the phase velocity is approximately constant (suggested by Figure 5b), then  $V_g$  equals the phase velocity. For the double-peaked wave observations, typical values are  $V \sin \theta = 4$  km/s, phase velocity is 150 km/s, which indicates that  $\Delta k/k < 0.1$ .

To show in more detail how the double peaks merge into a single spectral peak, as  $\Delta k/k$  increases, computer-generated signals, composed of gyrotronically distributed sine waves that were Doppler shifted into the DE 1 reference frame, were made for three different values of  $\Delta k/k$  corresponding to 0.02, 0.04, and 0.08. The signals had power levels and spectral characteristics similar to the double-peaked harmonic shown in Figure 2b. Since the inferred wavelengths of these waves are larger than the  $E_x$  antenna length, the signals were composed of the following sum of sine waves:

$$\Phi(t) = \mathbf{e}_{\text{boom}}(t) \cdot \sum_n \mathbf{E}_n \cos((\omega(\mathbf{k}_n) - \mathbf{k}_n \cdot \mathbf{V})t + \phi_n) \quad (3)$$

Here  $\Phi(t)$  is the Doppler-shifted signal detected in the DE 1 reference frame. The symbol  $\mathbf{e}_{\text{boom}}(t)$  is a unit vector that points in the direction of the  $E_x$  antenna.

The signals are composed of 200 sine wave components. Each component was assigned a randomly chosen phase ( $\phi_n$ ) and perpendicular wave number in the range  $|k_{\perp} - k_{\perp 0}| \leq \Delta k$ . A plot of the perpendicular wave numbers, for the

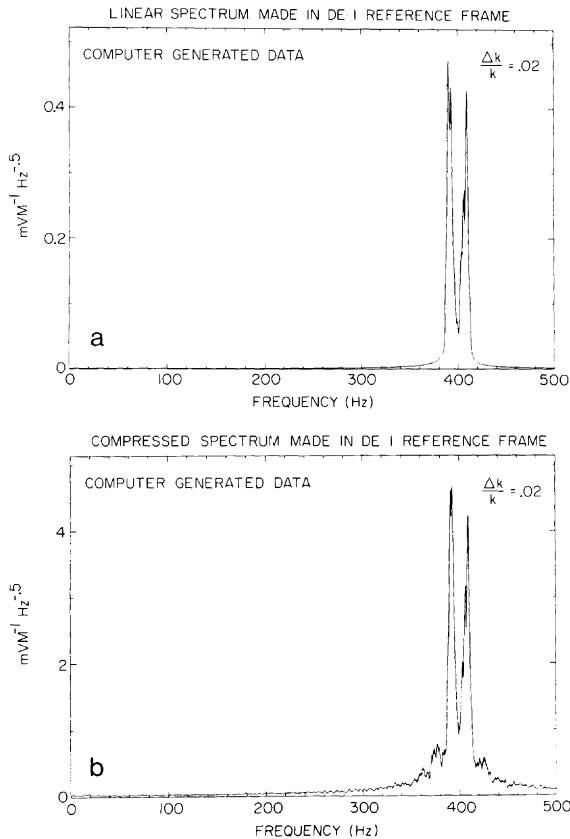


Fig. 8. Spectrums of computer-generated wave data are shown that are Doppler shifted into the DE 1 frame of reference for the case  $\Delta k/k = 0.02$ . (a) The spectrum of the signal produced by a linear receiver; (b) the spectrum of the signal that is logarithmically compressed.

case  $\Delta k/k = 0.02$ , is shown in Figure 7. The frequency of each wave number was determined by  $\omega(k_{\perp}) = \omega(k_{\perp 0}) + \mathbf{V}_g \cdot (\mathbf{k}_{\perp} - \mathbf{k}_{\perp 0})$ . The relative electric field for each component was determined by a Gaussian profile centered at  $k_{\perp} = k_{\perp 0}$  with a half width  $\Delta k$ . For each case the computer-generated signal covered a period of time equal to one satellite spin period.

The spectrums of the computer-generated signal for the case  $\Delta k/k = 0.02$  are shown in Figures 8a and 8b. The spectrum shown in Figure 8a would correspond to a frequency spectrum generated by a linear receiver, but the wideband receiver nonlinearly compresses the signal. To check the distortion of the signal caused by the nonlinear compression, a computer model of the logarithmic compression was made. The signal after compression is shown in Figure 8b. The spectrum of the computer-generated signal shows low-amplitude sidebands similar to low-amplitude sidebands observed in the real data (Figure 2b). The separation between the double peaks (Figures 8a and 8b) is the same value as that predicted by (1).

The spectrums of computer-generated signals for the cases when  $\Delta k/k = 0.04$  and  $0.08$  are shown in Figures 9a and 9b, respectively. The double peaks can still be clearly observed (Figure 9a) when  $\Delta k/k$  is set equal to 0.04, but they merge

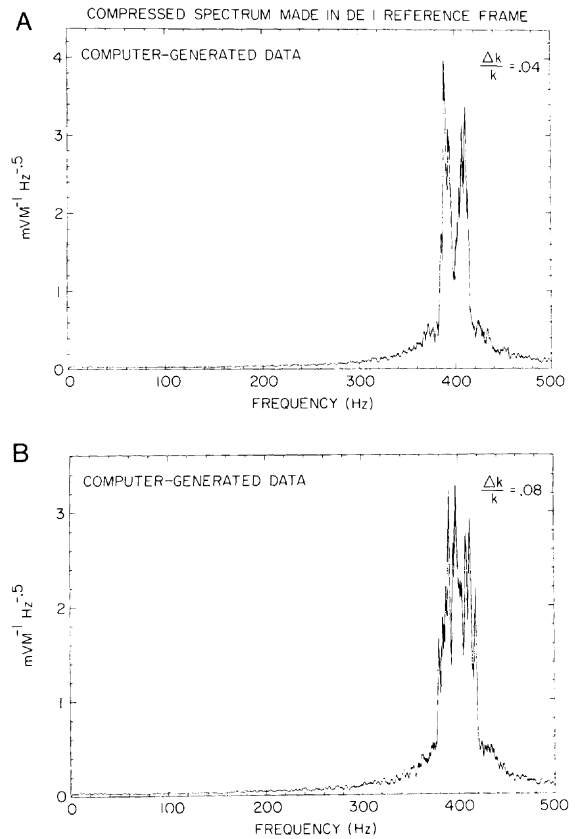


Fig. 9. Spectrums of computer-generated wave data are shown that are Doppler shifted into the DE 1 frame of reference for the cases (a)  $\Delta k/k = 0.04$  and (b)  $\Delta k/k = 0.08$ .

into a single spectral peak (Figure 9b) when  $\Delta k/k$  is set equal to 0.08. The computer model of the merging of the double peaks is in agreement with condition (2) as expected.

The only evidence we have which indicates that  $\Delta k/k$  is small for double-peaked events, compared to other events, arises from comparisons of the rms electric field amplitudes. The rms electric fields associated with double-peaked  $H^+$  cyclotron harmonics are typically weaker by a factor of 4 than the rms electric fields associated with other  $H^+$  cyclotron harmonics at similar altitudes. The smaller electric field of the double-peaked events suggests that these events are closer to marginal stability (i.e., zero growth rate) than the larger-amplitude, single-peaked harmonic emissions. Therefore one would expect that the growth rate is near zero for the double-peaked harmonics.

However, it should be pointed out that other low-intensity events like the one occurring from 035306 to 035350 UT on June 1 do not exhibit double-peaked harmonics. This apparent inconsistency could possibly be explained by a number of factors. The value of  $\Delta k/k$  is probably dependent on various factors other than the electric field strength, such as the plasma density, composition, temperatures, etc., all of which can be quite variable. The marginal stability argument given above is a starting point for which a more complete theory based on the growth, propagation, and saturation of these waves is needed. Also, other spectral broadening

mechanisms (for example, the spatial and temporal coherence of the waves) can also be important in obscuring the Doppler effect.

In the above analysis it was assumed that the plasma flow velocity ( $V_{\text{flow}}$ ) is much less than the satellite velocity ( $V_{\text{sat}}$ ). But if  $V_{\text{flow}}$  is larger or of the same order of magnitude as  $V_{\text{sat}}$ , the plasma flow velocity must be taken into account since it is reasonable to assume that the waves are gyrotropically distributed in the rest frame of the plasma. Let  $\phi_0$  be the angle between the projection of the  $E_x$  antenna perpendicular to the magnetic field and the projection of  $V_{\text{sat}} - V_{\text{flow}}$  perpendicular to the magnetic field (denoted by  $V_{\perp}$ ). Therefore the electric fields which make the maximum contribution to the wideband signal are Doppler shifted by  $\pm V_{\perp} \cos(\phi_0)/\lambda$ . Therefore (1) should be replaced by the following relationship:

$$\Delta f = 2V_{\perp} \cos(\phi_0)/\lambda \quad (4)$$

As the angle  $\phi_0$  increases toward  $90^\circ$ ,  $\Delta f$  decreases and the contribution made to the wideband signal by waves that would yield only a small Doppler shift is enhanced. Therefore the double peaks become less pronounced and gradually merge into a single peak as  $\phi_0$  approaches  $90^\circ$ .

One uncertainty in any method of analyzing the Doppler effect is the determination of the flow velocity of the plasma. The component of the plasma flow velocity perpendicular to the magnetic field is determined primarily by the  $\mathbf{E} \times \mathbf{B}$  drift. The parallel component of the flow velocity is relatively unimportant to the spreading of the harmonics but adds a Doppler shift ( $<0.1$  Hz) to the spectrum.

The  $E_x$  antenna measures an electric field intensity during the June 1 event which gives a value of 1.85 km/s for the component of the  $\mathbf{E} \times \mathbf{B}$  drift perpendicular to both the magnetic field and satellite velocity. This measurement gives the east-west component of the flow velocity. Unfortunately, the low plasma density and short length of the  $E_z$  antenna makes it impossible to determine the other component of the  $\mathbf{E} \times \mathbf{B}$  drift, which is the north-south component perpendicular to  $\mathbf{B}$ . Along the auroral field lines the north-south component is usually smaller than the east-west component.

Assuming the north-south component is negligible for the June 1 event, the  $x$  component (refer to Figure 6) of  $V_{\text{sat}} - V_{\text{flow}}$  is 3.75 km/s and the  $y$  component (east-west) is 1.85 km/s. Therefore the angle that  $V_{\perp}$  makes with projection of the  $E_x$  antenna perpendicular to the magnetic field is  $\phi_0 = 26^\circ$ . This means that the wavelengths in Table 1 could be underestimated by about 10%. If the north-south component is as large as the east-west component, the estimated uncertainty in determining the wavelength is about 30%.

There are no clear observations of double-peak emissions occurring in the spectra of electrostatic  $H^+$  cyclotron wave events (in which just the fundamental and lower harmonics are excited). In the majority of the electrostatic  $H^+$  cyclotron wave events, single-peaked harmonics are observed. The typical rms electric field amplitudes associated with these events are about a factor of 4 larger than the typical amplitudes observed for  $H^+$  cyclotron harmonic waves. Therefore  $\Delta k/k$  is probably larger for electrostatic  $H^+$  cyclotron waves and double-peaked harmonics are less likely to occur. Figure 10 shows a spectrum of an electrostatic  $H^+$  cyclotron wave event that occurred on January 4, 1984, at 1438:50 UT (the event is discussed by Peterson et al. [1988])

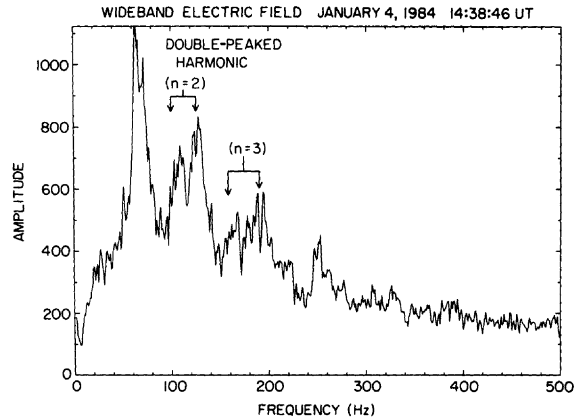


Fig. 10. A spectrum of the wideband electric field signal taken over the interval 1438:46–1438:58 on January 4, 1984. The fundamental peaks slightly above the hydrogen cyclotron frequency ( $f_{H^+} = 60$  Hz).

in which the second and third harmonics could be interpreted as being double peaked.

If Doppler spreading is the dominate broadening mechanism for electrostatic  $H^+$  cyclotron waves, assuming that  $\lambda$  is proportional to  $n^{-1}$ , the ratio of the half width of the second harmonic to the half width of the first harmonic should be about 2. Figure 11 shows a histogram of the ratio of the second harmonic to that of the first harmonic for a number of  $H^+$  cyclotron wave events. Clearly, the peak in the histogram lies closer to 1 instead of 2. This indicates that other broadening mechanisms, such as the coherence of the waves, play at least an equally important role for these events.

#### 4. CONCLUSION

Electrostatic  $H^+$  cyclotron harmonic emissions are often found to have double peaks associated with each harmonic. The separation in frequency of the double peaks is observed to increase with harmonic number. For the two cases found with double peaks occurring at low harmonic numbers ( $n \sim$

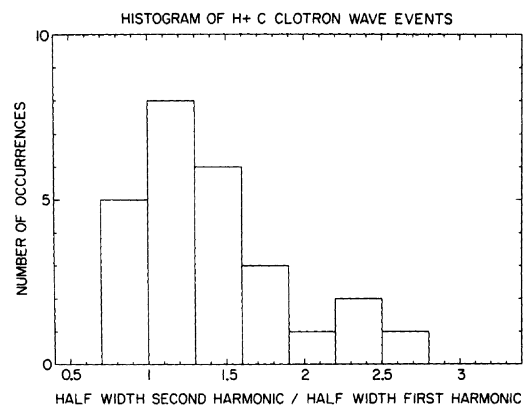


Fig. 11. A histogram of the ratio of the half width of the second harmonic to that of the first harmonic for a number of  $H^+$  cyclotron wave events, the peak in the histogram lies closer to 1 instead of 2.

3-7) the separation is observed to be proportional to the harmonic number. The waves occur below the lower hybrid frequency and are almost perpendicular to the magnetic field ( $k_{\parallel}/k_{\perp} < 0.2$ ).

The projection of the electric fields of these waves onto the  $E_x$  antenna, which rotates in the plane defined by the satellite velocity and magnetic field direction, favors waves traveling in a direction either parallel or antiparallel to the component of the satellite's velocity perpendicular to the magnetic field. Therefore a double-peaked spectrum can arise from the Doppler-shifted waves traveling close to the parallel and antiparallel direction, assuming that  $\Delta k/k$  is small and other broadening mechanisms are negligible.

The wavelength and phase velocity of the waves can be determined by measuring the separation between the peaks. The waves were found to have wavelengths of the order of 300 m and phase velocities of the order of a 150 km/s. The linear relationship between harmonic number and separation between the double peaks indicates that the phase velocity of these waves is approximately constant and independent of harmonic number.

In one case we showed that a substantial cold ( $T_{H^+} < 10$  eV above spacecraft potential)  $H^+$  ion component exists comprising at least 80% of the  $H^+$  density. Therefore the phase velocity is much greater than the background  $H^+$  thermal velocity. This observation suggests that the real part of the dispersion relationship can be approximated by the fluid limit, and therefore the phase velocity should be constant and close to the ion acoustic velocity. Unfortunately, no determination of the electron temperature could be made due to the failure of the plasma instrument which measures the electrons.

Assuming that the phase velocity ( $V_p$ ) is approximately constant, the spectral broadening due to the frequency dispersion relation is approximately  $V_p \cdot \Delta k$ . When this broadening is of the order of the separation of the peaks due to the Doppler shift, the double-peaked harmonics merge into a single spectral peak. We showed that  $\Delta k/k$  for these waves is less than 0.1. The only observational evidence that we have that suggests  $\Delta k/k$  is smaller for double-peaked ion cyclotron harmonic waves compared to a single-peaked ion cyclotron harmonic waves is that double-peaked ion cyclotron harmonic waves have amplitudes that are a factor of 4 smaller than amplitudes of single-peaked electrostatic ion cyclotron harmonic waves.

The major source of error in our estimates of the wavelength of these waves occurs because of the uncertainty in

determining the plasma flow velocity due to the short length of the  $E_z$  antenna. We estimate the uncertainty in determining the wavelength due to this cause to be about 30%.

*Acknowledgments.* We would like to thank M. Sugiura for the magnetometer data. We would also like to thank the referees for their constructive comments. The research at Lockheed was supported by NASA through contract NASS-28710, and the research at Iowa was supported by NASA grants NAG5-310, NGL 16-001-043, and NAGW-1488.

The Editor thanks M. K. Hudson and J. LaBelle for their assistance in evaluating this paper.

#### REFERENCES

- Andre, M., Electrostatic ion waves generated by ion loss-cone distributions in the magnetosphere, *Ann. Geophys.*, **86**, 241b, 1986.
- Chappell, C. R., The terrestrial plasma source: A new perspective in solar-terrestrial processes from Dynamics Explorer, *Rev. Geophys.*, **26**, 229, 1988.
- Kintner, P. M., On the distinction between electrostatic ion cyclotron waves and ion cyclotron harmonic waves, *Geophys. Res. Lett.*, **7**, 585, 1980.
- Kintner, P. M., M. C. Kelly, and S. F. Moser, Electrostatic hydrogen cyclotron waves near one Earth radius in the polar magnetosphere, *Geophys. Res. Lett.*, **5**, 139, 1978.
- Koskinen, H. E. J., P. M. Kintner, G. Holmgren, B. Holback, G. Gustafsson, M. Andre, and R. Lundin, Observations of ion cyclotron harmonic waves by the Viking satellite, *Geophys. Res. Lett.*, **14**, 459, 1987.
- Persoon, A. M., D. A. Gurnett, W. K. Peterson, J. H. Waite, Jr., J. L. Burch, and J. L. Green, Electron density depletions in the nightside auroral zone, *J. Geophys. Res.*, **93**, 1871, 1988.
- Peterson, W. K., E. G. Shelley, S. A. Boardsen, D. A. Gurnett, B. G. Ledley, M. Sugiura, T. E. Moore, and J. H. Waite, Jr., Transverse ion energization and low-frequency plasma waves in the mid-altitude auroral zone: A case study, *J. Geophys. Res.*, **93**, 11,405, 1988.
- Shawhan, S. D., D. A. Gurnett, and D. L. Odem, The plasma wave and quasi-static electric field instrument (PWI) for Dynamics Explorer-A, *Space Sci., Instrum.*, **5**, 535, 1981.
- S. A. Boardsen, NASA Marshall Space Flight Center, Code ES53, Building 4481, Huntsville, AL 35812.
- D. A. Gurnett, Department of Physics and Astronomy, University of Iowa, Iowa City, IA 52242.
- W. K. Peterson, Research and Development, Lockheed, 3251 Hanover Street, Palo Alto, CA 94304.

(Received April 24, 1989;  
revised December 27, 1989;  
accepted December 27, 1989.)